HDO abundance in the envelope of the solar-type protostar IRAS 16293-2422

Parise, B.; Dishoeck, E.F. van

Astronomy
&
Astrophysics

HDO abundance in the envelope of the solar-type protostar IRAS 16293–2422[*]

B. Parise[1], E. Caux[1], A. Castets[2], C. Ceccarelli[3], L. Loinard[4], A. G. G. M. Tielens[5], A. Bacmann[2], S. Cazaux[6], C. Comito[7], F. Helmich[5,8], C. Kahane[3], P. Schilke[7], E. van Dishoeck[9], V. Wakelam[2], and A. Walters[1]

[1] Centre d'Étude Spatiale des Rayonnements, BP 4346, 31028 Toulouse Cedex 04, France
   e-mail: parise@cesr.fr
[2] Observatoire de Bordeaux, BP 89, 33270 Floirac, France
[3] Laboratoire d'Astrophysique de l'Observatoire de Grenoble, BP 53, 38041 Grenoble Cedex 9, France
[4] Centro de Radioastronomía y Astrofísica, Universidad Nacional Autónoma de México, Apartado Postal 72-3 (Xangari),
   58089 Morelia, Michoacán, Mexico
[5] Kapteyn Astronomical Institute, University of Groningen, PO Box 800, 9700 AV Groningen, The Netherlands
[6] INAF, Osservatorio Astrofisico di Arcetri, Largo Enrico Fermi 5, 50125 Firenze, Italy
[7] Max-Planck-Institut für Radioastronomie, Auf dem Hügel 69, 53121 Bonn, Germany
[8] SRON National Institute for Space Research, Landleven 12, 9747 AD Groningen, The Netherlands
[9] Leiden Observatory, PO Box 9513, 2300 RA Leiden, The Netherlands

Abstract. We present IRAM 30 m and JCMT observations of HDO lines towards the solar-type protostar IRAS 16293−2422. Five HDO transitions have been detected on-source, and two were unfruitfully searched for towards a bright spot of the outflow of IRAS 16293−2422. We interpret the data by means of the Ceccarelli et al. (1996) model, and derive the HDO abundance in the warm inner and cold outer parts of the envelope. The emission is well explained by a jump model, with an inner abundance $x_{\rm in}^{\rm HDO} = 1 \times 10^{-7}$ and an outer abundance $x_{\rm out}^{\rm HDO} \leq 1 \times 10^{-9}$ (3σ). This result is in favor of HDO enhancement due to ice evaporation from the grains in the inner envelope. The deuteration ratio HDO/H$_2$O is found to be $f_{\rm in} = 3\%$ and $f_{\rm out} \leq 0.2\%$ (3σ) in the inner and outer envelope respectively and therefore, the fractionation also undergoes a jump in the inner part of the envelope. These results are consistent with the formation of water in the gas phase during the cold prestellar core phase and storage of the molecules on the grains, but do not explain why observations of H$_2$O ices consistently derive a H$_2$O ice abundance of several 10^{-5} to 10^{-4}, some two orders of magnitude larger than the gas phase abundance of water in the hot core around IRAS 16293−2422.

Key words. ISM: molecules – stars: formation – stars: individual: IRAS 16293−2422

1. Introduction

The field of molecular deuteration has seen, in recent years, a burst of new studies, both observational and theoretical, since the discovery of large amounts of doubly deuterated formaldehyde (about 10% with respect to the main isotopomer) in the low mass protostar IRAS 16293−2422 (hereinafter IRAS 16293, Ceccarelli et al. 1998, 2001). Following this discovery, other doubly or triply deuterated molecules have been detected having similarly high D/H enhancements: ammonia (Roueff et al. 2000; Loinard et al. 2001; van der Tak et al. 2002;

Lis et al. 2002), methanol (Parise et al. 2002, 2004) and hydrogen sulfide (Vastel et al. 2003).

Triggered by these observations, new models were developed to account for the large observed D/H molecular ratios (Roberts & Millar 2000a,b; Rodgers & Charnley 2003), with partial success. Nonetheless, it was soon understood that the key to obtain large molecular deuteration is cold and CO depleted gas, as confirmed by the observations towards a sample of pre-stellar cores (Bacmann et al. 2003) and predicted by the afore mentioned models. A step forward in the comprehension of the deuteration process has been the observation of a very large amount of H$_2$D$^+$ in the pre-stellar core L1544, where very likely H$_2$D$^+$/H$_3^+$ $\sim$ 1 (Caselli et al. 2003), after its first detection in the low mass protostar NGC1333 IRAS4A (Stark et al. 1999). This observational study triggered new models of gas phase chemistry, which take into account all deuterated isotopomers of H$_3^+$ (Roberts et al. 2003; Walmsley et al. 2004).

---

[*] Based on observations with the IRAM 30 m telescope in Spain and with The James Clerk Maxwell Telescope, operated by The Joint Astronomy Centre on behalf of the Particle Physics and Astronomy Research Council of the United Kingdom, the Netherlands Organisation of Scientific Research, and the National Research Council of Canada.

The comparison between model predictions and observations is much improved in this last class of models, also supported by the recent detection of D_2H^+ (Vastel et al. 2004).

Molecules like formaldehyde and methanol are almost certainly grain-surface products, specifically products of successive CO hydrogenation during the cold dark cloud phase. When a newly formed star heats up its environment, these species are released into the gas phase because of the ice mantle evaporation (Charnley et al. 1992; Caselli et al. 1993; Charnley et al. 1997; Tielens & Rodgers 1997). Therefore, their large deuteration must also occur on the grain surfaces (e.g. Ceccarelli et al. 2001; Parise et al. 2002, 2004). Note that fractionation ratios of 0.3, 0.06 and 0.01 have been measured for CH_2DOH, CHD_2OH and CD_3OH respectively (Parise et al. 2004), so that one would naively expect similarly large HDO/H_2O ratios if water forms on the grains simultaneously with methanol. However, searches in low-mass sources where large D_2CO/H_2CO ratios have been measured have shown no HDO ices at a very low limit ($\leq 2\%$; Parise et al. 2003). While early analysis of the ISO-SWS spectrum of the high-mass protostars W33A and NGC7538 IRS9 led to HDO/H_2O_{ice} ratios of respectively 8×10^{-4} and 10^{-2} (Teixeira et al. 1999), reanalysis of this data and supporting ground-based data also derived upper limits of 1% (Dartois et al. 2003). One possibility is that the process of water formation on ices is intrinsically unfavorable to water deuteration because of the involved routes or, alternatively, it is possible that gas phase and solid phase observations do not probe the same components (see also the discussion in Parise et al. 2003). Whatever the answer is, it is clear that the process of molecular deuteration will not be fully mastered until this last puzzle has a satisfying solution.

The HDO fractionation has already been measured in a number of high-mass hot cores. The HDO/H_2O ratio was observed to be $3–6 \times 10^{-4}$ in a sample of galactic hot cores (Jacq et al. 1990). Subsequent observations derived similar fractionation ratios in other high-mass YSO (Gensheimer et al. 1996; Helmich et al. 1996; Comito et al. 2003).

In order to address the fundamental question of water versus formaldehyde and methanol deuteration, we carried out observations of five HDO vapor lines towards the low mass protostar IRAS 16293, to measure the HDO/H_2O ratio *in the gas phase*, and compare it with the observed fractionations for formaldehyde (Loinard et al. 2000), and methanol (Parise et al. 2004). Note that IRAS 16293 is one of the few sources where the water abundance profile has been derived, based on ISO-LWS observations (Ceccarelli et al. 2000a). Several studies have shown that the envelope of IRAS 16293 consists of an outer envelope where the molecular abundances are similar to molecular cloud ones, and an inner envelope where several species have enhanced abundances because of grain mantle evaporation (Ceccarelli et al. 2000a,b, 2001; Schöier et al. 2002, 2004; Cazaux et al. 2003). It is worth emphasizing that, in this respect, IRAS 16293 is fully representative of solar-mass Class 0 sources (Maret et al. 2004; Jørgensen et al. 2004). Finally, Stark et al. (2004) recently reported the detection of the HDO ground transition towards IRAS 16293 and derived a HDO abundance of $\sim 10^{-10}$ in the cold region of the
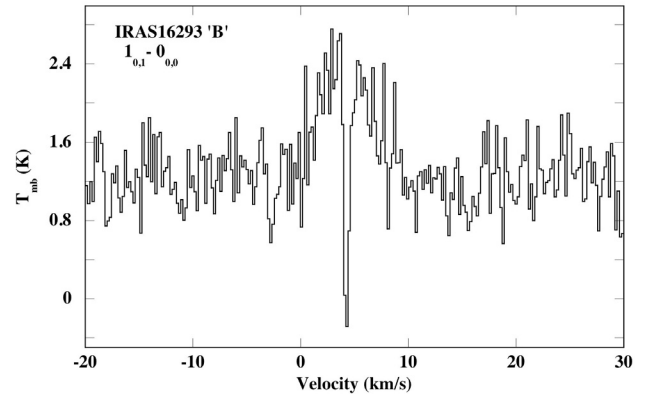

Fig. 1. HDO 464.9 GHz line observed on-source (IRAS 16293 "B") at the JCMT.

envelope. These authors report only upper limits of higher-lying HDO transitions, which prevented an accurate estimate of the HDO abundance in the warm region. We report here the detection of five HDO lines with energies up to 168 K, which allows a study of the HDO abundance in the inner envelope.

The article is organized as follows: the observations and results are presented in Sect. 2, the modeling and its uncertainties are described in Sect. 3, and the implications of the results are discussed in Sect. 4.

2. Observations and results

2.1. Observations

IRAS 16293 is known to be comprised of two components, "A" and "B", separated from one another by about 5 arcsec (Wootten 1989; Mundy et al. 1992). The observations were performed at the JCMT and at the IRAM 30 m telescopes on the IRAS 16293 "B" source at $\alpha(2000.0) = 16^h32^m22.6''$, $\delta(2000.0) = -24°28'33''$. The resolution of the observations reported here is never sufficient to resolve the binary system. The emission of both components is included in the beam used for the observations (10″ to 33″). Some of these data have been obtained from an unbiased spectral survey of IRAS 16293 conducted at IRAM and JCMT by a European Consortium.

The ground ($1_{0,1}-0_{0,0}$) transition of HDO at $\nu = 464.9$ GHz was observed on July 26th, 1999 with the JCMT near the summit of Mauna Kea in Hawaii, USA. The observations were made with the single-sideband dual-polarization W receiver. Each polarization of the receiver was connected to a unit of an autocorrelator providing a bandwidth of 250 MHz for a spectral resolution of 156 kHz. At 465 GHz, this yields a velocity resolution of about 0.1 km s^{-1}. The observations were made in position switching mode with the OFF position at offset $\Delta\alpha = -180''$, $\Delta\delta = 0''$ from our nominal position. The spectrum obtained is presented in Fig. 1. The narrow self absorption is due to the surrounding cloud (see also Stark et al. 2004).

All other observations were performed with the IRAM 30 m telescope on Pico Veleta near Granada, in Southern Spain. To probe where the location of the HDO emission originates (warm envelope of the source or outflow?), we observed in addition a position in the flow, at $\Delta\alpha = -39''$, $\Delta\delta = 0''$ from the

Table 1. HDO lines parameters. The three sections are for the three aimed positions. In italics, we quoted the results published by Stark et al. (2004).

Observing date	Telescope	Transition	Frequency GHz	Eup K	Beam ″	T_{int} min	T_{sys} K	δv km s^{-1}	rms mK	T_{peak} mK	Δv km s^{-1}	$\int T_{mb}dv$ K km s^{-1}
IRAS 16293 "B" (α(2000.0) = 16^{h}32^{m}22.6″, δ(2000.0) = −24°28′33″)
01/20/04	IRAM	$1_{1,0}–1_{1,1}$	80.578	46.8	33	42	190	1.2	10	81	4.9	0.40
01/25/04	IRAM	$3_{1,2}–2_{2,1}$	225.897	167.7	12	60	650	1.3	12	245	6.2	1.7
03/29/00	IRAM	$2_{1,1}–2_{1,2}$	241.561	95.3	11	35	880	0.4	62	400	6.6	2.0
02/03/04	IRAM	$2_{2,0}–3_{1,3}$	266.161	157.3	10	68	820	1.4	14	75	3.0	0.21
07/26/99	JCMT	$1_{0,1}–0_{0,0}$	464.924	22.3	11	140	3000	0.2	290	1200	6.0	5.5
Flow (α(2000.0) = 16^{h}32^{m}20″, δ(2000.0) = −24°28′33″)
03/09/04	IRAM	$1_{1,0}–1_{1,1}$	80.578	46.8	33	40	230	0.58	14	–	6.0*	< 0.05*
03/09/04	IRAM	$2_{1,1}–2_{1,2}$	241.561	95.3	11	40	950	0.4	38	–	6.0*	< 0.01*
IRAS 16293 "A" (α(2000.0) = 16^{h}32^{m}22.85″, δ(2000.0) = −24°28′35.5″)
1998	*JCMT*	*$1_{0,1}–0_{0,0}$*	*464.924*	*22.3*	*11*	*–*	*–*	*–*	*–*	*1000*	*5.9*	*6.0*
2001	JCMT	$3_{1,2}–2_{2,1}$	225.897	167.7	21	120	715	0.83	18	87	6.5	0.61
2001	JCMT	$2_{1,1}–2_{1,2}$	241.561	95.3	20	96	690	0.78	23	112	5.4	0.62

* For the outflow observations, since no linewidth can be determined, a mean width of 6 km s^{-1} was assumed. The data have been smoothed to the velocity resolution δv given in Col. 8, used to determine the rms noise. "–" means the information is not available or cannot be derived. The last 3 observations are from Stark et al. (2004).

on-source nominal position. This position was chosen, first because it is the location of one of the brightest emissions of the outflow (CO, Stark et al. 2004), and second to make sure that we do not intercept emission from the warm envelope of the protostar in the large 33″ beam of the 30 m at 80.6 GHz.

For on-source observations, we used the beam-switching observing mode, with a symmetric switch of 240″ from the nominal center of the source. For the flow observations, we used the position-switching observing mode, with a switch of $\Delta\alpha = -3600″$, $\Delta\delta = 0″$ to ensure a reference position well outside the outflow. Two receivers were always used simultaneously, connected to a unit of an autocorrelator or filter bank backend.

The spectral resolutions used, angular resolutions of the telescope, integration times (ON+OFF) and system temperatures are quoted in Table 1 for both JCMT and 30 m observations. Pointing and focus were regularly checked using planets or strong quasars, providing a pointing accuracy of about 3″ for both telescopes.

All intensities reported in this paper are expressed in units of main-beam brightness temperature, using the efficiencies given on the JCMT and 30 m web sites (http://jach.hawaii.edu/JACpublic/JCMT/home.html and http://www.iram.fr/IRAMES/index.htm).

2.2. Results

The obtained spectra are presented in Figs. 1 and 2 and show that on the flow position the two searched lines are not detected at all while all observed lines are detected on-source. The intensity of the HDO ground transition at 464.9 GHz is very similar to what Stark et al. (2004) observed at a position centered
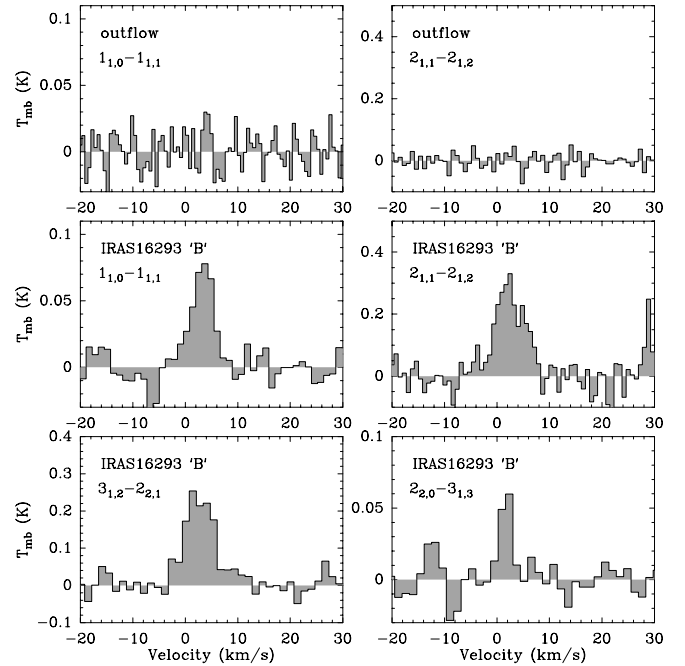
Fig. 2. HDO lines observed at the 30 m on the outflow and on-source (IRAS 16293 "B").

on IRAS 16293 "A", 5″ away from our IRAS 16293 "B" position, where they find an integrated flux about 10% larger than ours. This is not the case for the 225.9 and 241.6 GHz lines, for which Stark et al. (2004) reported very low upper limits (≤120 mK km s^{-1} assuming a 6 km s^{-1} linewidth). We retrieved from the JCMT database the original observations performed by Stark on the 225.9 and 241.6 GHz lines and reduced the
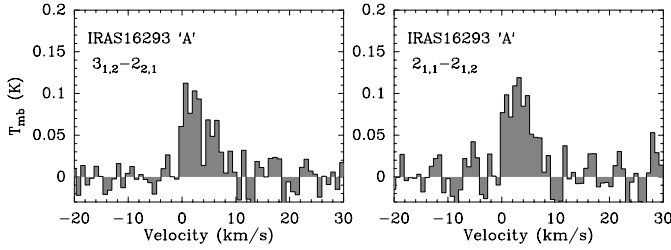
Fig. 3. Rereduction of the HDO 225.9 and 241.6 GHz lines observed by Stark et al. in 2001 at JCMT on IRAS 16293 "A".

Fig. 4. $x_{\mathrm{in}}^{\mathrm{HDO}}$ and $x_{\mathrm{out}}^{\mathrm{HDO}}$ contours (1, 2 and 3σ) for the reduced χ^2. The "+" corresponds to the best fit model. $x_{\mathrm{in}}^{\mathrm{HDO}}$ is very well constrained, $(1 \pm 0.3 \times 10^{-7})$, as well as the upper limit of $x_{\mathrm{out}}^{\mathrm{HDO}}$ ($\leq 1 \times 10^{-9}$, 3σ).

data again. The results are shown in Fig. 3, where the two HDO lines are clearly seen at the 100 mK level, which is in good agreement with our result taking into account the beam dilution in the JCMT telescope. Our results are also in good agreement with the observation of the 241.6 GHz line reported by van Dishoeck et al. (1995).

Table 1 summarizes the results of all the observational sets. Because of the presence of an absorption component, which is obvious for the ground transition and may be present for other lines, we defined the integrated intensity for all lines as the sum of all channels in the velocity range [−5, 10]. The quoted linewidths are those of a Gaussian fit to the data. The δv is the spectral resolution obtained after Hanning windowing (if any) in Figs. 1 to 3.

Except for the 266.2 GHz line, which is the noisiest one, the observed linewidths are broad – ∼6 km s^{-1} – and therefore should come mainly from either the infalling inner warm envelope or from the outflow, rather than from the cold envelope. Furthermore, the observed intensity for both 225.9 and 241.6 GHz HDO lines is very different at JCMT and at the 30 m. This can be explained if the emission of these lines comes from a very small region, more diluted in the JCMT beam than it is in the 30 m beam. If we assume the size of the emitting region to be small with respect to the 30 m beam (Ceccarelli et al. 2000a modelled 2″), we expect a flux about 4 times larger in the 30 m beam, very similar to what we observe (2.8 at 225.9 GHz and 3.2 at 241.6 GHz). We attribute the residual disagreement to slightly different positions between the Stark (IRAS 16293 "A") and our (IRAS 16293 "B") observations.

If the HDO emission arises from a very small region, this argues in favour of the warm envelope for the origin of the emission, rather than from the outflow. This is also strongly suggested by the non-detection of both 80.6 and 241.6 GHz lines towards the outflow at the 30 m. We will therefore model the observed HDO line emission assuming the lines originate in the envelope of the protostar.

3. Modeling and discussion

3.1. Modeling

The structure of the envelope of IRAS 16293 was derived by Ceccarelli et al. (2000a) using H$_2$O lines observed with ISO-SWS and ISO-LWS, and substantially confirmed by the subsequent analysis of Schöier et al. (2002). The water
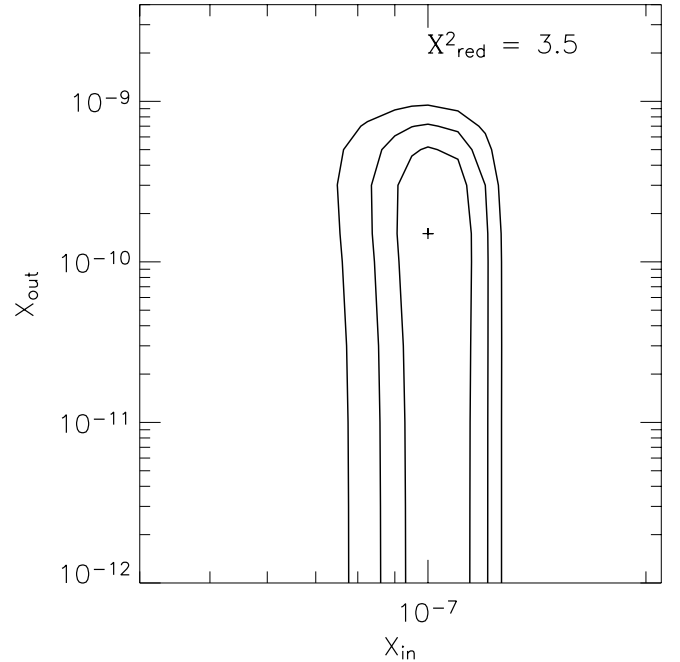
emission was modeled in terms of a jump model (Ceccarelli et al. 1996, hereinafter CHT96), where the abundances of water in the inner part of the envelope ($T \geq 100$ K, evaporation temperature of the icy grain mantles) and in the outer part ($T \leq 100$ K) are two free parameters. The derived inner abundance was $x_{\mathrm{in}}^{\mathrm{H_2O}} = 3 \times 10^{-6}$ (with respect to H$_2$) and the outer abundance $x_{\mathrm{out}}^{\mathrm{H_2O}} = 5 \times 10^{-7}$ (Ceccarelli et al. 2000a).

Studies of the spatial distribution of formaldehyde in IRAS 16293 have shown that the structure may be more complex than a single step function, as a further jump may be present at around 50 K, due to evaporation of CO-rich ices (Ceccarelli et al. 2001; Schöier et al. 2004). Given the low number of observed transitions, we will consider here the simple case of a single jump. The abundance derived in the outer region will therefore likely be an average over the regions where CO is depleted and starts to evaporate.

For the analysis of the present HDO data, we adapted the time-dependent CHT96 model to compute the HDO line emission at a given time. The collisional coefficients were taken from Green et al. (1989), and the details of the model are reported in Parise, Ceccarelli & Maret (2004). We adopted the temperature and density structure derived by Ceccarelli et al. (2000a) for the envelope and left the inner and outer HDO abundances as free parameters. We then performed a χ^2 analysis for $x_{\mathrm{in}}^{\mathrm{HDO}}$ ranging from 1×10^{-9} to 1×10^{-6} and for $x_{\mathrm{out}}^{\mathrm{HDO}}$ ranging from 1×10^{-12} to 1×10^{-8}. The best model fitting the 5 observed lines on-source corresponds to $x_{\mathrm{in}}^{\mathrm{HDO}} = 1 \times 10^{-7}$ and $x_{\mathrm{out}}^{\mathrm{HDO}} = 1.5 \times 10^{-10}$, and gives a reduced χ^2 of 3.5. Figure 4 presents the contours delimiting the 1σ, 2σ and 3σ confidence intervals (corresponding respectively to $\chi_{\mathrm{red}}^2 = \chi_{\mathrm{min}}^2 + 1.18$, $\chi_{\mathrm{min}}^2 + 2.70$ and $\chi_{\mathrm{min}}^2 + 5.06$ as relevant for 3 degrees of freedom). The inner abundance is very well
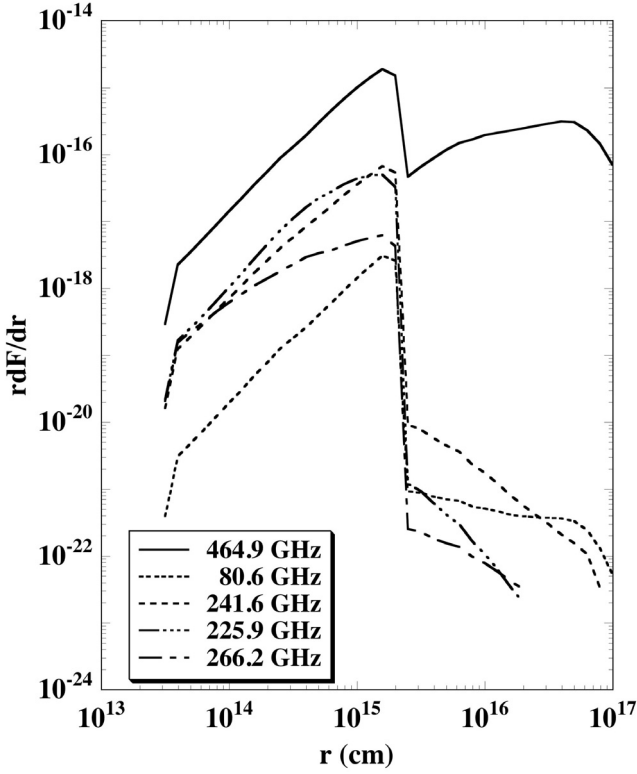
Fig. 5. Radial emission profiles of the five HDO lines, using $x_{\rm in}^{\rm HDO} = 1 \times 10^{-7}$ and $x_{\rm out}^{\rm HDO} = 1.5 \times 10^{-10}$.

constrained, while the data only provide an upper limit on the outer abundance. The lower limit on the outer abundance is poorly constrained, because the only transition constraining it is the ground transition at 464.9 GHz. Figure 5 shows the radial profile of the emission of the five HDO lines computed with $x_{\rm in}^{\rm HDO} = 1 \times 10^{-7}$ and $x_{\rm out}^{\rm HDO} = 1.5 \times 10^{-10}$. It is clear on this figure that only the ground transition has a contribution from the outer envelope, and even more that the bulk of the emission originates in the inner part of the envelope.

We also performed the same analysis with only the 3 lines observed on IRAS 16293 "A" at JCMT (225.9, 241.6 and 464.9 GHz). The resulting abundances are $x_{\rm in}^{\rm HDO} = 1.1 \times 10^{-7}$ and $x_{\rm out}^{\rm HDO} \leq 1 \times 10^{-9}$ (3σ), compatible with the results found on IRAS 16293 "B". Note that with their analysis, Stark et al. (2004) estimate a constant HDO abundance of 3×10^{-10} throughout the envelope, compatible with the abundance we derive in the outer envelope. On the contrary, they do not find an abundance jump in the warm inner envelope, presumably because they only used the ground transition to constrain it.

3.2. Uncertainties of the model

Following the discussion in Maret et al. (2004), the values of the inner and outer abundances derived by our model can be uncertain for several reasons that we review below:

– To test the influence of the outer abundance in the derivation of the inner abundance, we arbitrarily imposed an outer abundance one order of magnitude greater than the derived abundance (simulating e.g. an extreme absorption

of the ground transition by foreground clouds). We then constrained the inner abundance without using the ground transition. The best fit is still obtained for the same value of $x_{\rm in}^{\rm HDO}$ and we can thus conclude that this result is robust regardless of any foreground absorption of the ground transition.

– To check the validity of the jump model, we ran a model with a constant HDO abundance throughout the envelope. The best fit is obtained in this case for an abundance of 1.2×10^{-9}, but the fit is very poor, yielding a reduced χ^2 of 40. We conclude from this analysis that a jump model is required to account for the observed HDO emission.

– In order to test the influence of the evaporation temperature (assumed to be 100 K in the present study), we also ran the model for an evaporation temperature of 50 K. The model using this new input parameter poorly fits our observations. Indeed, the best fit is obtained with a reduced χ^2 of 42 to be compared to the value of 3.5 when the evaporation temperature is 100 K. This analysis is in good agreement with the measured evaporation temperature of water-rich ices (Sandford & Allamandola 1990).

– As noted previously, the 464.9 GHz linewidth is about 6 km s^{-1}, which would suggest that it originates from the inner warm region. To check if this is true, we ran the model with a very low value of the outer HDO abundance, $x_{\rm out}^{\rm HDO} = 7.5 \times 10^{-12}$, i.e. with no enhancement with respect to the cosmic abundance (D/H$_{\rm ISM} = 1.5 \times 10^{-5}$, Linsky et al. 1998) and using $x_{\rm out}^{\rm H_2O} = 5 \times 10^{-7}$, (Ceccarelli et al. 2000a). In this last case, the best fit corresponds to $x_{\rm in}^{\rm HDO} = 1.05 \times 10^{-7}$, the bulk of the ground HDO transition originates in the inner region, and the model underestimates the observed flux by only 15%. Therefore, the 6 km s^{-1} linewidth of the ground HDO transition is consistent with our model as most of it originates in the inner warm region. Of course, the presence of the narrow self-absorption feature suggests that while most of the 464.9 GHz emission originates from the warm inner envelope, some HDO has to be present in the outer cold, absorbing envelope.

Thus, Fig. 6 shows the ratios between the observations on IRAS 16293 "B" and the model predictions for three cases: a) the jump model with $x_{\rm in}^{\rm HDO} = 1 \times 10^{-7}$ and $x_{\rm out}^{\rm HDO} = 1.5 \times 10^{-10}$; b) the case with a constant abundance throughout the envelope ($x_{\rm in}^{\rm HDO} = x_{\rm out}^{\rm HDO} = 1.2 \times 10^{-9}$); and c) the case where the HDO abundance in the outer envelope is $x_{\rm out}^{\rm HDO} = 7.5 \times 10^{-12}$.

All the checks done strengthen the fact that the observations are consistent with the previously derived HDO inner and outer abundances. They are summarized in Table 2. These values lead, when compared to the H$_2$O abundances determined by Ceccarelli et al. (2000a), to the fractionation ratios indicated in Table 2. Note that these H$_2$O abundances are also relatively uncertain. In particular, the inner abundance could be underestimated as it is derived from optically thick lines. Although Ceccarelli et al. (2000a) provide an upper limit on $x_{\rm in}^{\rm H_2O}$ of 3.5×10^{-6}, future observations of water lines with the Herschel-HIFI spectrometer are needed to reduce the uncertainties on the water distribution.
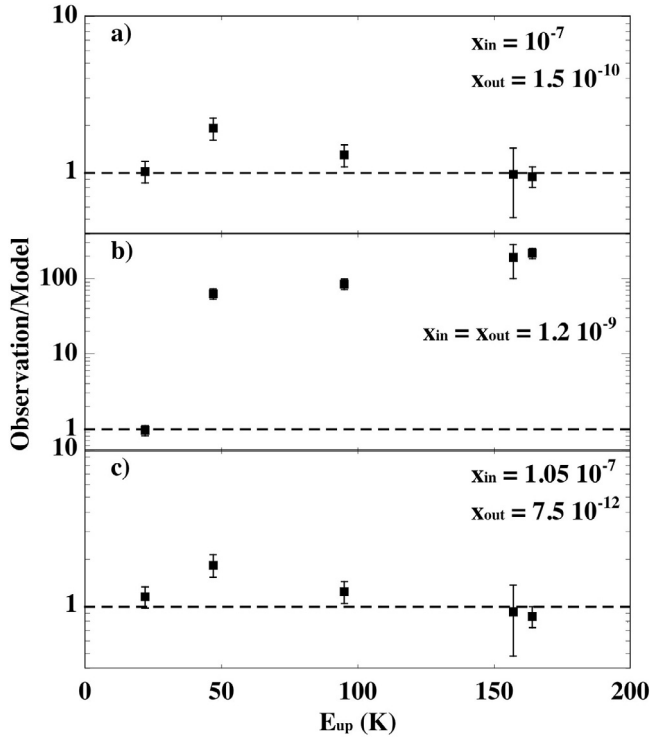
Fig. 6. Ratios between the observations on IRAS 16293 "B" and the model predictions for three cases: **a)** the jump model with $x_{in}^{HDO} = 1 \times 10^{-7}$ and $x_{out}^{HDO} = 1.5 \times 10^{-10}$, **b)** a model with a constant abundance throughout the envelope, and **c)** a case of no enhancement at all of the emission associated with the outer envelope (see text).

Table 2. Summary of the results of the modeling.

	Inner envelope	Outer envelope
x^{HDO}	1×10^{-7}	$\leq 1 \times 10^{-9}$
x^{H_2O*}	3×10^{-6}	5×10^{-7}
HDO/H$_2$O	3%	$\leq 0.2\%$ (3σ)

* Ceccarelli et al. (2000a).

3.3. Discussion

These results clearly show that the abundance of HDO undergoes a jump in the inner part of the envelope, where the ices evaporate from the grains, and that, even more strikingly, the fractionation also undergoes such a jump. This is not in agreement with the results of Stark et al. (2004), who found an equal HDO abundance in the inner and outer envelope of the source and a HDO/H$_2$O ratio of 0.15% in the inner warm envelope and 2 to 20% in the outflow. Regarding the abundance in the inner and in the outer envelope, our analysis of several lines demonstrates that indeed there is a region where the HDO abundance exhibits a jump. On the contrary, we do not have any observational evidence that HDO is associated with the outflow as we do not detect any emission in the position of the outflow (see Fig. 2 and Table 1). However, we cannot totally rule out that at least part of the HDO emission comes from an interaction of the envelope with the outflow, as suggested by Stark et al. (2004).

The deuteration fractionation of water derived in the inner part of the envelope is lower by one order of magnitude than the fractionation of methanol (30% for CH$_2$DOH, Parise et al. 2002, 2004) and formaldehyde (15%, Loinard et al. 2000). This result is consistent with the non detection of solid HDO towards low-mass protostars which exhibit a high deuteration of formaldehyde in the gas phase (Parise et al. 2003). The present analysis confirms that water is indeed less deuterated than formaldehyde and methanol in the hot core of low-mass protostars.

Comito et al. (2003) derived a fractionation of 6.4×10^{-4} in the hot core region of the SgrB2 complex, similar to the water fractionation HDO/H$_2$O = $(2-6) \times 10^{-4}$ found in the high-mass protostar W3 by Helmich et al. (1996). Such low values of the HDO fractionation (a few 10^{-4}) have also been derived in some high-mass star forming regions by the pioneering work of Jacq et al. (1990). Our results show that the water fractionation in the solar-type protostar IRAS 16293 is much higher than what is observed in high-mass protostars, as already pointed out for the formaldehyde (Loinard et al. 2002) and methanol fractionation (Jacq et al. 1993; Parise et al. 2002, 2004).

The jump by more than a factor of 10 in the fractionation of water in the region where mantles evaporate suggests that the fractionation processes are substantially different in the two regions:

- In the outer envelope, where the dust temperature is not high enough to efficiently evaporate the molecules stored in grain mantles, the fractionation might reflect current gas-phase deuteration processes. In the gas-phase scheme, the deuteration is driven by reactions with H$_2$D$^+$. This can lead to a water fractionation enhancement of up to several percent when the temperature is very low ($T \sim 10$ K, Roberts et al. 2000b; Roberts et al. 2004), because of the endothermicity of the reaction H$_2$D$^+$ + H$_2$ → H$_3^+$ + HD, enhancing the H$_2$D$^+$/H$_3^+$ ratio relatively to the HD/H$_2$ ratio. In the outer envelope, temperatures span from ~ 10 K to 100 K, and the measured fractionation is thus characteristic of a medium warmer than 10 K, for which fractionation drops very quickly with respect to 10 K (cf. Fig. 2b of Roberts et al. 2000b). The fractionation value ($\leq 0.2\%$) that we derive is thus in agreement with this gas phase scheme.

- On the contrary, in the inner envelope, the fractionation may probe the deuteration of the molecules formed during an earlier cold phase when CO depletion was extreme, as observed presently in some prestellar cores (Caselli et al. 1999; Bacmann et al. 2002, 2003; Crapsi et al. 2004). These molecules are stored in the grain mantles that evaporate once the protostar heats its surroundings.

In the inner envelope, the difference between the fractionation of water on the one hand and formaldehyde and methanol on the other hand is, as discussed by Parise et al. (2003), a strong constraint to chemical models. Because of the low efficiency of its production in the gas phase and in view of its high abundance in icy mantles, methanol is believed to be formed on the grains by active grain surface chemistry, by successive hydrogenations of CO (Tielens 1983; Charnley et al. 1992, 1997).

If water is also produced by active grain chemistry, the lower fractionation of water compared with methanol suggests that either there is a selective incorporation of deuterium in the methanol route (successive hydrogenations/deuterations of CO, resulting in the production of formaldehyde and methanol) rather than in the water route, or water is not formed simultaneously with methanol.

Such segregation of ices is indicated by solid CO observations towards a sample of low-mass protostars showing evidence that 60% to 90% of solid CO is in the form of pure CO-ice (Tielens et al. 1991; Boogert et al. 2002; Pontopiddan et al. 2003). Likewise, observations of solid CO_2 also provide evidence for separate ice components along the same line of sight, although, in this case, this is generally attributed to the segregation of mixed $H_2O/CH_3OH/CO_2$ ices upon warm up by a newly formed star (Ehrenfreund et al. 1998, 1999; Gerakines et al. 2000; Boogert et al. 2000).

Perhaps the water ice observation refers to a global property of molecular clouds while the methanol-rich ices are more localized to regions of star formation. Indeed, studies of the ice abundance suggest that H_2O-ice appears wherever $A_V > 3$ mag (Whittet et al. 1988; Chiar et al. 1995), while methanol ice is rarely seen in dark clouds (Chiar et al. 1996).

One of the possibilities discussed by Parise et al. (2003) can be ruled out by these new observations. Indeed, the possibility that H_2O is condensed out on the grains after a shock during the cloud phase (as suggested by Bergin et al. 1999) can be rejected in the case of IRAS 16293 as the deuteration in such a scheme would be lower than a few 10^{-3}, i.e. at least 10 times smaller than the fractionation we derive in the inner warm envelope.

Another possibility is that water is produced in the gas phase at low temperature during the prestellar core phase before it is stored in the grain mantles. The gas phase model predictions of Roberts et al. (2000b) seem to be in agreement with this scheme. Indeed, the water fractionation is expected to reach a few percent in a gas at 10 K and density $n = 5 \times 10^4$ cm^{-3}, even without considering CO depletion (see Fig. 3 of Roberts et al. 2000b). The water abundance is predicted to be nearly 10^{-6} in this case, i.e. only a factor of 3 below the abundance $x_{in}^{H_2O}$ derived by Ceccarelli et al. (2000a). Both H_2O and present HDO observations in the warm inner envelope may thus be consistent with the formation of water in the gas phase, the dust playing only a passive role in maintaining the fractionation at its cold value during storage of the molecules.

While such a model would be consistent with our gas phase observations of H_2O and HDO (e.g., absolute abundance as well as fractionation behavior), observations of ices consistently derive a H_2O ice abundance of 10^{-4} in high-mass protostars (Whittet et al. 1988; Smith et al. 1989; Gibb et al. 2004), and 5×10^{-5} in low-mass protostars (Boogert et al. 2004), at least one order of magnitude larger than the gas phase abundance of H_2O in the hot core around IRAS 16293. Such high abundances of H_2O ice are generally thought to reflect active grain surface chemistry, e.g. hydrogenation of atomic oxygen on grain surface (Tielens & Hagen 1982; Jones et al. 1990). This discrepancy between the hot core H_2O abundance in IRAS 16293 and the general H_2O ice abundance may merely reflect a unique situation for this source but that solution is not very satisfactory. In particular, IRAS 16293 is often considered to be the template solar-type class 0 protostar and, indeed, it shares many properties of class 0 sources (e.g. Ceccarelli et al. 2000b; Maret et al. 2004). In a way, all models − including the grain surface chemistry origin of H_2O − have to face this same problem of the difference in the hot core and solid state H_2O abundance. If the gas phase composition of hot cores really reflects the evaporation of ices, the H_2O abundance would be expected to be much higher. The much lower gaseous H_2O abundance in the hot core − as compared to the H_2O-ice abundance towards protostars − was already noted by Ceccarelli et al. (2000a). They attributed this discrepancy to a breakdown of spherical symmetry when the size approaches the core-rotation radius (∼30 AU) and the presence of a disk. In this disk, much of the water may be frozen out. At the same time, the disk is also not accounted for in the studies of the total gas column density. Likely, the HDO/H_2O ratio in the inner part is less sensitive to these uncertainties. The HIFI heterodyne instrument on Herschel will provide further insight into these issues.

4. Conclusion

Five HDO lines have been detected towards the solar-type protostar IRAS 16293"B" using the IRAM 30 m and JCMT telescopes. Two lines (80.6 and 241.6 GHz) were unfruitfully searched for at the 30 m towards a bright spot of the outflow of IRAS 16293.

We modeled the emission on-source with the CHT96 jump model, and derived the HDO abundance in the inner and outer parts of the envelope to be $x_{in}^{HDO} = 1 \times 10^{-7}$ and $x_{out}^{HDO} \leq 1 \times 10^{-9}$, in agreement with HDO enhancement due to the ices' evaporation from the grains in the inner envelope.

The water fractionation also undergoes a jump as we obtained $f_{in} = 3\%$ and $f_{out} \leq 0.2\%$ in the inner and outer envelope, respectively. These results are consistent with the formation of water in the gas phase during the cold prestellar core phase and storage of the molecules on the grains. They do not explain why H_2O observations of ices consistently derive a H_2O ice abundance of several 10^{-5} to 10^{-4}, some two orders of magnitude larger than the gas phase abundance of water in the hot core around IRAS 16293.

References

Bacmann, A., Lefloch, B., Ceccarelli, C., et al. 2002, A&A, 389, L6
Bacmann, A., Lefloch, B., Ceccarelli, C., et al. 2003, ApJ, 585, L55
Bergin, E. A., Neufeld, D. A., & Melnick, G. J. 1999, AJ, 510, L145
Boogert, A. C. A., Tielens, A. G. G. M., Ceccarelli, C., et al. 2000, A&A, 360, 683

Boogert, A. C. A., Pentoppidan, K. M., Lahuis, F., et al. 2004, ApJS, 154, 359

Boogert, A. C. A., Hogerheijde, M. R., & Blake, G. A. 2002, ApJ, 568, 761

Caselli, P., Hasegawa, T. I., & Herbst, E. 1993, ApJ, 408, 548

Caselli, P., Walmsley, C. M., Tafalla, M., Dore, L., & Myers, P. C. 1999, ApJ, 523, L165

Caselli, P., van der Tak, F. F. S., Ceccarelli, C., & Bacmann, A. 2003, A&A, 403, L37

Ceccarelli, C., Hollenbach, D. J., & Tielens, A. G. G. M. 1996, ApJ, 471, 400

Ceccarelli, C., Castets, A., Loinard, L., Caux, E., & Tielens, A. G. G. M. 1998, A&A, 338, L43

Ceccarelli, C., Castets, A., Caux, E., et al. 2000a, A&A, 355, 1129

Ceccarelli, C., Loinard, L., Castets, A., Tielens, A. G. G. M., & Caux, E. 2000b, A&A, 357, L9

Ceccarelli, C., Loinard, L., Castets, A., et al. 2001, A&A, 372, 998

Charnley, S. B., Tielens, A. G. G. M., & Millar, T. J. 1992, ApJ, 399, L71

Charnley, S. B., Tielens, A. G. G. M., & Rodgers, S. D. 1997, ApJ, 482, L203

Chiar, J. E., Adamson, A. J., Kerr, T. H., & Whittet, D. C. B. 1995, ApJ, 455, 234

Chiar, J. E., Adamson, A. J., & Whittet, D. C. B. 1996, ApJ, 472, 665

Crapsi, A., Caselli, P., Walmsley, C. M., et al. 2004, A&A, 420, 957

Dartois, E., Thi, W.-F., Geballe, T. R., et al. 2003, A&A, 399, 1009

Ehrenfreund, P., Dartois, E., Demyk, K., & D'Hendecourt, L. 1998, A&A, 339, L17

Ehrenfreund, P., Kerkhof, O., Schutte, W. A., et al. 1999, A&A, 350, 240

Gerakines, P. A, Moore, M. H., & Hudson, R. L. 2000, A&A, 357, 793

Gibb, E. L., Whittet, D. C. B., Boogert, A. C. A., & Tielens, A. G. G. M. 2004, ApJS, 151, 35

Green, S. 1989, ApJS, 70, 813

Helmich, F. P., van Dishoeck, E. F., & Jansen, D. J. 1996, A&A, 313, 657

Jacq, T., Walmsley, C. M., Henkel, C., et al. 1990, A&A, 228, 447

Jacq, T., Walmsley, C. M., Mauersberger, R., et al. 1993, A&A, 271, 276

Jones, A. P., Duley, W. W., & Williams, D. A. 1990, QJRAS, 31, 567

Jørgensen, J. K., Schöier, F. L., & van Dishoeck 2004, A&A, 416, 603

Linsky, J. L., Wilson, T. L., & Rood, R. T. 1998, SSR, 84, 309

Lis, D. C., Roueff, E., Gerin, M., et al. 2002, ApJ, 571, 55

Loinard, L., Castets, A., Ceccarelli, C., et al. 2000, A&A, 359, 1169

Loinard, L., Castets, A., Ceccarelli, C., Caux, E., & Tielens, A. G. G. M. 2001, ApJ, 552, L163

Loinard, L., Castets, A., Ceccarelli, C., et al. 2002, P&SS, 50, 1205

Maret, S., Ceccarelli, C., Caux, E., et al. 2004, A&A, 416, 577

Mundy, L. G., Wootten, A., Wilking, B. A., Blake, G. A., & Sargent, A. I. 1992, ApJ, 385, 306

Parise, B., Ceccarelli, C., Tielens, A. G. G. M., et al. 2002, A&A, 393, L49

Parise, B., Simon, T., Caux, E., et al. 2003, A&A, 410, 897

Parise, B., Castets, A., Herbst, E., et al. 2004, A&A, 416, 159

Parise, B., Ceccarelli, C., & Maret, S. 2004, in preparation

Pontoppidan, K. M., Fraser, H. J., Dartois, E., et al. 2003, A&A, 408, 981

Roberts, H., & Millar, T. J. 2000a, A&A, 361, 388

Roberts, H., & Millar, T. J. 2000b, A&A, 364, 780

Roberts, H., Herbst, E., & Millar, T. 2003, ApJ, 591, 41

Roberts, H., Herbst, E., & Millar, T. J. 2004, A&A, 424, 905

Rodgers, S. D., & Charnley, S. B. 2003, ApJ, 585, 355

Roueff, E., Tiné, S., Coudert, L. H., et al. 2000, A&A, 354, L63

Sandford, S. A., & Allamandola, L. J. 1990, Icarus, 87, 188

Schöier, F. L., Jörgensen, J. K., van Dishoeck, E. F., & Blake, G. A. 2002, A&A, 390, 1001

Schöier, F. L., Jörgensen, J. K., van Dishoeck, E. F., & Blake, G. A. 2004, A&A, 418, 185

Smith, R. G., Sellgren, K., & Tokunaga, A. T. 1989, ApJ, 344, 413

Stark, R., van der Tak, F. F. S., & van Dishoeck, E. F. 1999, ApJ, 521, L67

Stark, R., Sandell, G., Beck, S. C., et al. 2004, ApJ, 608, 341

Teixeira, T. C., Devlin, J. P., Buch, V., & Emerson, J. P. 1999, A&A, 347, L19

Tielens, A. G. G. M., & Hagen, W. 1982, A&A, 114, 245

Tielens, A. G. G. M. 1983, A&A, 119, 177

Tielens, A. G. G. M., Tokunaga, A. T., Geballe, T. R., & Baas, F. 1991, ApJ, 381, 181

van der Tak, F. F. S., Schilke, P., Müller, H. S. P., et al. 2002, A&A, 388, 53

van Dishoeck, E. F., Blake, G. A., Jansen, D. J., & Groesbeck, T. D. 1995, ApJ, 447, 760

Vastel, C., Phillips, T. G., Ceccarelli, C., & Pearson, J. 2003, ApJ, 593, L97

Vastel, C., Phillips, T. G., & Yoshida, H. 2004, ApJ, 606, L127

Walmsley, C. M., Flower, D. R., & Pineau des Forêts, G. 2004, A&A, 418, 1035

Whittet, D. C. B., Bode, M. F., Longmore, A. J., et al. 1988, MNRAS, 233, 321

Wootten, A. 1989, ApJ, 337, 858